New Journal of Physics
The open access journal at the forefront of physics

Deutsche Physikalische Gesellschaft DPG
IOP Institute of Physics

Published in partnership with: Deutsche Physikalische Gesellschaft and the Institute of Physics

OPEN ACCESS

RECEIVED
12 July 2017

REVISED
16 November 2017

ACCEPTED FOR PUBLICATION
23 November 2017

PUBLISHED
5 January 2018

PAPER

Superradiant to subradiant phase transition in the open system Dicke model: dark state cascades

Michael Gegg, Alexander Carmele, Andreas Knorr and Marten Richter[1]

Institut für Theoretische Physik, Nichtlineare Optik und Quantenelektronik, Technische Universität Berlin, Hardenbergstr. 36, EW 7-1, D-10623 Berlin, Germany

[1] Author to whom any correspondence should be addressed.

E-mail: michael.gegg@tu-berlin.de **and** marten.richter@tu-berlin.de

Keywords: Dicke model, collective effects in quantum optics, superradiance and subradiance, quantum entanglement, specific phase transitions

Abstract

Collectivity in ensembles of atoms gives rise to effects like super- and subradiance. While superradiance is well studied and experimentally accessible, subradiance remains elusive since it is difficult to track experimentally as well as theoretically. Here we present a new type of phase transition in the resonantly driven, open Dicke model that leads to a deterministic generation of subradiant states. At the transition the system switches from a predominantly superradiant to a predominantly subradiant state. Counterintuitively, the cavity decay is the crucial parameter for subradiant state generation and not the individualizing process of spontaneous decay. The observed effect is thus a cavity assisted generation of subradiant quantum coherences. Clear experimental signatures for the effect are presented and entanglement properties are discussed. Letting the system relax into the ground state generates a cascade of dark Dicke states, with dark state populations up to unity. Furthermore we introduce a collectivity measure that allows to quantify collective behaviour.

1. Introduction

The open (and closed) system Dicke model has been a work horse in quantum optics and beyond for decades [1–28]. Current research on Dicke model based systems includes novel laser-like systems [22], phase transitions [19, 26], quantum information and super/subradiance [14, 17, 23, 24, 27, 29]. In recent years superradiance has been investigated with respect to entanglement [23] and subradiance for its prospects to store quantum information [24, 29]. The Dicke model assumes N identical two-level systems, interacting with a bosonic cavity mode.

Investigating subradiant effects in a consistent open system theory was not feasible for a long time since in a straight forward approach the master equation scales exponentially in the number N of two-level systems. This renders full simulations even for small N impossible. Subradiance appears already for few particles, however the behaviour towards more emitters cannot be modelled using the full exponential approach. Common limits and approximations for both analytical and numerical treatments addressing this problem are also not suited to study subradiance even for moderate N [4–10, 14, 17]. Usually for superradiance total spin conservation (explained below) is assumed, entirely neglecting subradiant states. This reduces the numerical complexity to $\sim N^2$ [5] or sometimes even allows analytic solutions [8–10, 17]. However ubiquitous phenomena in real systems like decay processes and pure dephasing break the conservation of total spin symmetry. Therefore, both realistic treatments and subradiant effects require a different methodology.

The formal permutation symmetry of the master equation itself allows, under some simple hypothesis on the initial state, to reduce the complexity from an exponential scaling in N to a polynomial scaling $\sim N^3$, even without total spin conservation [11, 22, 30–34]. This makes exact calculations for moderate emitter numbers feasible and removes constraints imposed by assumptions and approximations. Furthermore the method can be applied to any set of permutation symmetric multi-level systems [33, 35].

In this work we investigate the steady state population of subradiant states through decay and pure dephasing processes—both do not conserve the total spin. The system is driven by an external laser and increasing the driving strength results in a non-equilibrium phase transition in the steady state behaviour. Counterintuitively, the cavity lifetime determines the population of the subradiant states: for short cavity lifetimes (bad cavity limit) subradiant states are always suppressed by quantum coherence. Contrary, increasing the cavity lifetime results in a collective, quantum coherent amplification of population in subradiant states. Thus the quality of the collective behaviour of the two-level systems is drastically changed by tuning the cavity lifetime, even though the cavity decay does not break the total spin symmetry and thus does not couple different Dicke subspaces. The individual spontaneous emission process is a necessary requirement for the population of subradiant Dicke states. However the associated decay rate has *no* influence on the population behaviour of the subradiant states in typical parameter regimes for laboratory quantum optics and quantum information setups, such as quantum dots, NV centres, Rydberg atoms, etc. The cavity quality is the only parameter determining the quality of the collective effects in the present system. Therefore the coherences of the subradiant states are only formed through the cavity degrees of freedom. The observed effect is thus a cavity assisted generation of subradiant quantum coherences. The quantitative discussion of the collective behaviour of the system in the steady state is enabled by the introduction of a collectivity measure.

In the bad cavity limit this setup resembles the scenario known as cooperative resonance fluorescence, including individualization, which has been studied in the past using mean field theory and phase space methods/large system size limits [4, 6, 9, 10]. This removes an essential part of quantum coherent effects [36]. These studies found bistable behaviour similar to absorptive optical bistability. This stems from a competition between collective and individual behaviour. These older studies focused on mean excitations and two-level system correlation functions—we place the focus on investigating superradiant and especially subradiant effects, which requires a careful treatment of the quantum coherences in the system. Furthermore hyperradiance of two individual non symmetric atoms, but also with an individual spontaneous decay as considered here, is introduced and studied using a radiance witness in [28].

Experimentally accessible signatures of this effect and entanglement properties via spin squeezing are discussed. Switching off the external driving once the steady state is reached, the subsequent relaxation into the ground state forms a long-lived cascade of dark Dicke states. This results in a simple, deterministic protocol for dark state preparation with populations close to unity under the influence of dephasing, with applications in quantum information storage.

2. Model system

We consider the usual Dicke model with an additional classical optical, cw field E driving all TLS identically. Driving is necessary since subradiant states are excited states. In a frame rotating at the external laser frequency, using the rotating wave approximation the system Hamiltonian reads

$$H = \hbar\Delta_0 b^\dagger b + \hbar\Delta_1 J_{11} + \hbar g\,(J_{10} b + J_{01} b^\dagger) + \hbar E (J_{10} + J_{01}), \tag{1}$$

where Δ_0, Δ_1 are the mode and TLS detuning, g is the TLS-mode coupling, E is the optical driving, b, $b^\dagger$ are photonic operators and $J_k = \sum_i \sigma_k^i$, $k = 11,\ 10,\ 01,\ 00$ are the collective spin operators. Excited and ground state of the individual TLS i are $|1\rangle_i$, $|0\rangle_i$. The spin operators, in the Bra and Ket representation, are $\sigma_{11}^i = |1\rangle_i\langle 1|_i$, $\sigma_{10}^i = |1\rangle_i\langle 0|_i$, $\sigma_{01}^i = |0\rangle_i\langle 1|_i$ and $\sigma_{00}^i = |0\rangle_i\langle 0|_i$. We assume resonant excitation field, cavity and TLS. Both cavity and TLS are subject to loss and dephasing, using Lindblad formalism [37]. The master equation reads

$$\partial_t \rho = \mathcal{L}\rho = \frac{\mathrm{i}}{\hbar}[\rho, H] + \mathcal{D}_{\mathrm{de}}(\rho) + \mathcal{D}_{\mathrm{pd}}(\rho) + \mathcal{D}_{\mathrm{ph}}(\rho). \tag{2}$$

The Lindblad dissipators describe decay processes like individual radiative and non-radiative decay $\mathcal{D}_{\mathrm{de}}(\rho) = \gamma/2\sum_i(2\sigma_{01}^i\rho\sigma_{10}^i - \sigma_{11}^i\rho - \rho\sigma_{11}^i)$, pure dephasing $\mathcal{D}_{\mathrm{pd}}(\rho) = \delta/2\sum_i(\sigma_z^i\rho\sigma_z^i - \rho)$ and cavity decay $\mathcal{D}_{\mathrm{ph}}(\rho) = \kappa/2(2b\rho b^\dagger - b^\dagger b\rho - \rho b^\dagger b)$, see figure 1(a). We use $\sigma_z^i = \sigma_{11}^i - \sigma_{00}^i$. All contributions to the master equation except $\mathcal{D}_{\mathrm{de}}$ and $\mathcal{D}_{\mathrm{pd}}$ are total spin preserving, (figure 1(b)). The total spin $l(l+1)$ is the eigenvalue of the $J^2 = (J_{10}J_{01} + J_{01}J_{10})/2 + J_z$ operator, with $J_z = 1/2\sum_i \sigma_z^i$. The value of l varies between $l_{\max} = N/2$ for the superradiant subspace and $l_{\min} = 0,\ 1/2$ for the (most) subradiant subspace. The J^2 and J_z eigenvalues determine the coupling strength of the multi TLS (Dicke) state to the cavity mode and the coherent, external drive. This coupling determines the rate of cavity photon generation as well as the pumping strength. The magnitude of the coupling strength distinguishes between superradiance and subradiance. For superradiant states the coupling strength scales superlinear in N, while for subradiant states the scaling is sublinear in N and some subradiant states are dark [38]. Dark means that the collective coupling to the cavity and the coherent, external drive of these states vanishes, meaning these states cannot decay via collective interactions e.g. by creating a cavity photon. However these states still decay into other states via the decay and dephasing processes

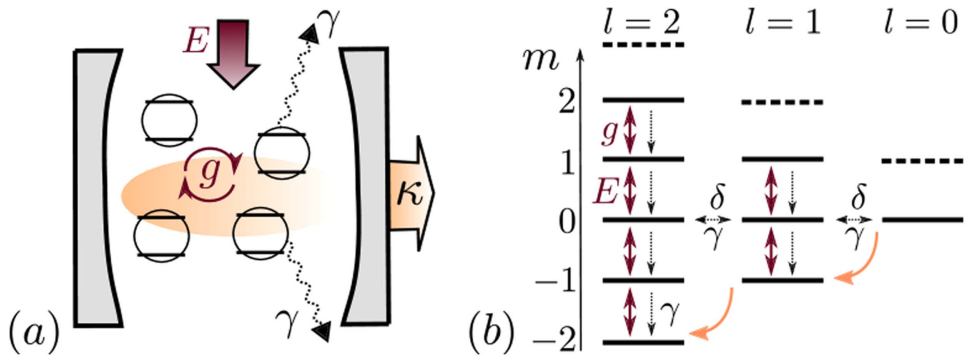

Figure 1. Illustrating the open Dicke model: (a) schematic representation of the system. (b) Dicke states for $N = 4$. The lowest state in each l subspace is dark—the lowest state in the superradiant $l_{\max} = N/2$ subspace is the ground state. The interactions are depicted: Hamiltonian part (purple,thick), dissipators $\mathcal{D}_{\text{de}}$ and $\mathcal{D}_{\text{pd}}$ (black,thin) and dark state cascade (orange,curved). Dashed lines indicate the additional states for $N = 5$ (with different values of m, l).

$\mathcal{D}_{\text{de}}$ and $\mathcal{D}_{\text{pd}}$ acting individually on the emitters, see figure 1(b). Generally the spin preserving contributions in the master equation (like equation (1)) generate quantum correlations leading to collective TLS behaviour (*both* super- and subradiance are collective effects) and the nonpreserving terms destroy correlations leading to individualization (all properties scale exactly linear in N). However only the spin nonpreserving contributions introduce coupling between superradiant and subradiant states, thus in order to prepare subradiant states an interplay of collectivity and individualization is necessary.

Based on these considerations the distinction of the behaviour of the system in this work is twofold: we distinguish between collective versus individual behaviour and superradiant versus subradiant behaviour. The latter are special cases of collective behaviour. This twofold distinction seems crucial when investigating super- and subradiance in the presence of dehasing and individual decay.

In the bad cavity limit ($\kappa \gg g$) equation (2) corresponds to the cooperative resonance fluorescence setup [4–6]. The system exhibits a non-equilibrium phase transition for increasing E for both total spin preserving and nonpreserving setups, where the nonpreserving setup was studied using mean field theory [4]. For longer cavity lifetimes κ the system more and more resembles the absorptive optical bistability setup [39] (instead of driving the TLS, in optical bistability the cavity is driven, opposed to figure 1(a)). In the range investigated in this work ($\kappa \sim g$) the clear distinction between cooperative resonance fluorescence and optical bistability breaks down, thus combining these distinct fields of quantum optics. Besides the steady state, density matrix states with very long lifetimes can exist in these systems, which lead to the observation of bistabilities in experiments with finite measurement time [40]. In some limits these lifetimes go to infinity, resulting in a second steady state. For optical bistability these long lifetimes are called tunnelling times [12, 41], more generally this phenomenon is called dissipative phase transition [42].

3. Permutation symmetric method

The formal permutation symmetry of the master equation allows the incorporation of the individual TLS decay and dephasing while having moderate numbers of TLS and photonic Fock states, since it reduces the number of relevant TLS Liouville space states from 4^N to $(N+1)(N+2)(N+3)/6$. This method was first introduced by Sarkar and Satchell in 1987 [11, 12] as the few emitter analogue to the widely used phase space methods in quantum optics, in particular the positive P representation [31, 43], which breaks down for $\leqslant$50 two-level systems [36]. The connection of this permutation symmetric method to the phase space methods can be seen from the fact that there are exactly $(N+1)(N+2)(N+3)/6$ distinct, linearly independent ordered products of the collective operators $J_{10}^p J_z^q J_{01}^r$ [31]. These operator products can also be used to expand the master equation in actual calculations [27, 31]. In recent years the permutation symmetric method has been independently rediscovered by different groups using different approaches [22, 26, 32, 33, 44, 45].

The states introduced in these methods may allow a more intuitive understanding of the processes in the system depending on the mathematical formulation. In the following we will use the formulation developed in [22, 33, 35]. For a permutation symmetric master equation the TLS density matrix is described by elements $\mathcal{P}[n, k, l]$ with $0 \leqslant n + k + l \leqslant N$. These elements describe the full density matrix and their number scales with $\propto N^3$. For element $\mathcal{P}[n, k, l]$ n of the N TLS are in a σ_{11} Liouville state, k are in a σ_{10} state and l in a σ_{01} state. σ_{01} and σ_{10} ($k \neq 0$ and/or $l \neq 0$) correspond to a quantum coherence/offdiagonal element in the individual density matrix. The different elements can be interpreted as follows: $\mathcal{P}[n, 0, 0]$ is the incoherent probability of

finding the N TLS system with n excited TLS. For instance preparing the system in a thermal state results in a thermal distribution in the $\mathcal{P}[n,\,0,\,0]$ densities, or preparing the system in the ground state is equivalent to $\mathcal{P}[0,\,0,\,0] = 1$ and zero for all other $\mathcal{P}[n,\,k,\,l]$. The elements $\mathcal{P}[n,\,k,\,l]$ for $k,\,l \neq 0$ describe quantum correlations and thus are constructed from the offdiagonal elements of the full density matrix, including inter-TLS coherences. For $k = l$ i.e. $\mathcal{P}[n,\,k,\,k]$ these elements are real valued but still represent offdiagonal density matrix elements/coherences between different TLS. The $\mathcal{P}[n,\,k,\,k]$ are collective quantum contributions and contribute to the *collective Dicke state population* of excited states in the system: more precise the $\mathcal{P}[n,\,k,\,k]$ distinguish collective Dicke state populations from classical, individual excited state populations in the open system, density matrix setting: the offdiagonal elements of the density matrix between different TLS are directly connected to the collective effects in the many emitter setup. In the following we will explain this relation in more detail and introduce a measure to distinguish collective Dicke behaviour from classical, individual behaviour in the presence of dephasing. For more details on the permutation symmetric variant used here and the density matrix elements $\mathcal{P}[n,\,k,\,l]$ please refer to appendix A and [33, 35, 46].

The photonic degrees of freedom are treated using the usual bosonic number states, that are cutoff at appropriate values in order to achieve convergence. Therefore the full calculations are carried out using the quantities $\mathcal{P}[n,\,k,\,l;\,m_l,\,m_r]$, including the photon degrees of freedom of the density matrix with an expansion in the $|m_l\rangle\langle m_r|$ elements. This is explained more formally in appendix A.

4. Collectivity measure

Investigating super- and subradiant states requires a suitable measure. Unfortunately computing the respective Dicke state populations is not sufficient for investigating collective effects and quantum coherence, if dephasing is present: Dicke states $|l,\,m\rangle$ are eigenstates of J^2 and J_z with corresponding quantum numbers $l(l+1)$, $0 \leqslant l \leqslant N/2$ and $|m| \leqslant l$. $l_{\max} = N/2$ defines the superradiant subspace and $l_{\min} = 0,\,1/2$ defines the (most) subradiant subspace, see figure 1(b). As an example consider the $N = 2$ Dicke (or Bell) states: the superradiant subspace consists of three states $|1,\,-1\rangle, |1,\,0\rangle, |1,\,+1\rangle$ while the subradiant subspace consists of a single dark state $|0,\,0\rangle$. First we calculate the population of the Dicke states: $\mathrm{tr}[|l,\,m\rangle\langle l,\,m|\rho] = \langle |l,\,m\rangle\langle l,\,m|\rangle = p(l,\,m)$ in the local basis. Using the permutation symmetric density matrix elements $\mathcal{P}[n,\,k,\,l]$ we can write these populations as

$$p(l,\,m) = a_0(l,\,m)\mathcal{P}[n,\,0,\,0] + a_1(l,\,m)\mathcal{P}[n-1,\,1,\,1]\,\ldots\,, \tag{3}$$

with $n = m + N/2$. In the presence of dephasing the elements $\mathcal{P}[n,\,k,\,k]$ for $k \neq 0$ experience dephasing. The $\mathcal{P}[n,\,k,\,k]$ represent quantum coherences between different TLS. If the dephasing is strong enough it will completely suppress quantum correlations, i.e. $\mathcal{P}[n,\,k,\,k] = 0$ for $k \neq 0$. This represents a completely incoherent mixture of TLS occupations. For varying numbers N of TLS, different $\mathcal{P}[n,\,0,\,0]$ distributions allow a large variety of populations in super- and subradiant states even if quantum coherences between different TLS are absent, since the relative size of the superradiant and subradiant Hilbert spaces vary for both N and n. Generally—when total spin non-conserving terms are included—the superradiant subspace population decreases, since for large N the superradiant subspace is very small compared to the full Hilbert space ($N+1$ versus 2^N). However without quantum coherences between different TLS ($\mathcal{P}[n,\,k,\,k],\;k \neq 0$) the label super- and subradiance becomes meaningless, since the inter-TLS quantum coherences are the signatures of the collectivity of the Dicke states and reflect the redistribution of oscillator strength through collective effects (phase locking). Thus—in the open Dicke model—$\mathcal{P}[n-k,\,k,\,k]$ are the key quantities that distinguish a super- or subradiant state from a classical, incoherent mixture of TLS population ($\mathcal{P}[i,\,j,\,k] = 0$ for $j,\,k \neq 0$). The decay process $\mathcal{D}_{\mathrm{de}}$ and the pure dephasing $\mathcal{D}_{\mathrm{pd}}$ act individually on every TLS and thus destroy the collectivity, resulting in incoherent mixtures.

To quantify the effect of collectivity and distinguish between collective (super- and subradiance) and individual (dipole moment scales linear in N) behaviour we introduce the ratio between the full Dicke subspace population and its incoherent part

$$R(l) = \frac{\sum_m p(l,\,m)}{\sum_m a_0(l,\,m)\mathcal{P}[m+N/2,\,0,\,0]}, \tag{4}$$

as a collectivity measure for the different Dicke subspaces l. $R(l) = 1$ holds if the influence of quantum correlations between the individual TLS on the subspace population is zero or negligible—the TLS act *individually*. $R(l) < 1/R(l) > 1$ holds if quantum correlations *suppress/increase* the respective subspace occupation—the TLS act *collectively*. $R(l)$ provides a reality check, since in any experiment dephasing is present and isolated Dicke subspaces (or states) never occur.

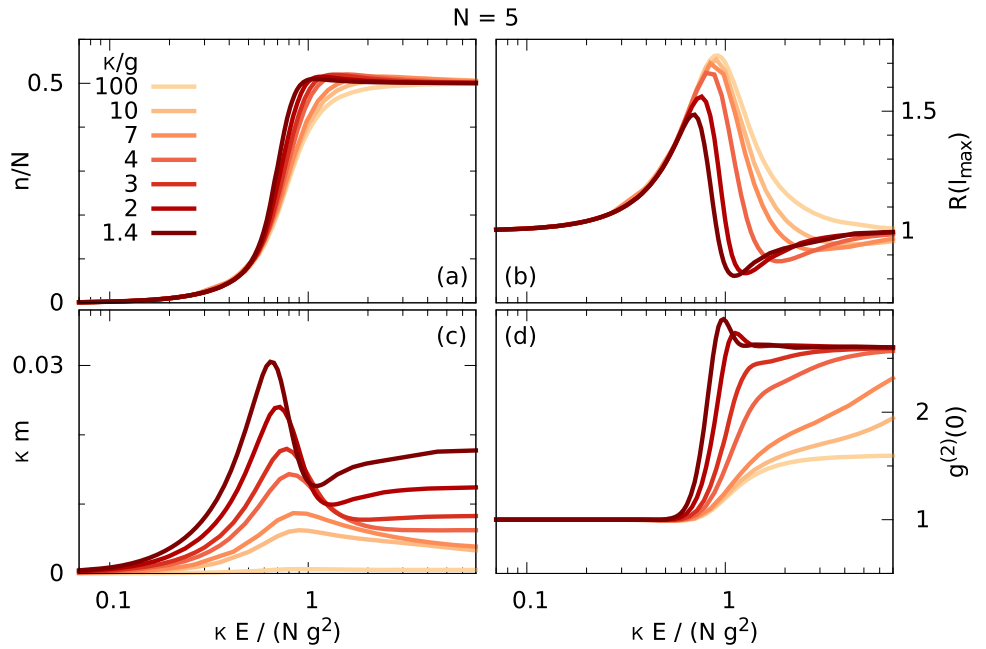

Figure 2. Leaving the bad cavity limit: variation of the external pumping strength for different ratios κ/g: (a) the normalized TLS excitation number $n/N = \langle J_{11}\rangle/N$, (b) the relative superradiant subspace occupation $R(l_{\max} = N/2)$, (c) the cavity output rate $\kappa m = \kappa\langle b^{\dagger}b\rangle$ and (d) the photonic second order correlation function $g^{(2)}(0)$: drastic qualitative change for κ/g approaching unity.

5. Results and discussion

We solve equation (2) with our computer library PsiQuaSP [35, 46] for master equations with reduced, polynomial scaling (see appendix A for a short introduction and [33] for more details). We use eigensolvers and time integration from PETSc and SLEPc [47–50].

We use $g = 5$ ps^{-1} throughout this work and $\gamma = 1.0$ ns^{-1} except for figures 5(c) and (d). Please note that ultra-strong coupling effects are not present in the investigated parameter range. There are two types of dephasing/individualization processes: spontaneous decay and pure dephasing. We first investigate the spontaneous decay and investigate the effects of pure dephasing later. Including small pure dephasing preserves all effects (see section 5.2 for a discussion).

5.1. Nature of the phase transition

In the steady state the most basic feature of the nonequilibrium phase transition is the change from the ground state to a half excited TLS state with increasing external driving field (figure 2(a)). The mean field theory expects a bistable behaviour [4], but in the full quantum treatment this is replaced by a slowing down in steady state convergence [12, 41] (see figure 4(b)). Increasing the cavity quality (decreasing the ratio between cavity decay rate and TLS-cavity coupling strength κ/g) makes the transition sharper but overall the effect does not change much. Contrary a drastic change is seen in the behaviour of the collectivity measure for the superradiant subspace $R(l_{\max} = N/2)$, figure 2 (b). While in the bad cavity limit the superradiant subspace population is always increased by collective effects ($R(l_{\max}) \geqslant 1$), we observe an increased suppression ($R(l_{\max}) < 1$) of the superradiant subspace for increasing cavity lifetime/quality. This is accompanied by a drastic increase of coherent cavity photons below and a pronounced bunching at moderate photon numbers above the phase transition (figures 2(c) and (d)). The maximum in the second order photon correlation function indicates the transition point from increased to suppressed superradiant subspace occupation. Please note that the cavity decay does not lead to an effective dephasing/individualization contribution for the TLS, thus the population of subradiant states through different cavity lifetimes is a highly nontrivial effect.

Above the phase transition collectivity favours the most subradiant subspace $l_{\min}$: the dependence of $R(l_{\max})$ on the number of TLS N, figure 3(a), shows a growing collective change in population of the superradiant subspace for increasing N. In figure 3(b) the ratio $R(l_{\max} - 2)$ is plotted—it switches from collective suppression below to collective increase above the transition (this subspace only exists for $N \geqslant 4$). However the collective increase in population decreases for increasing N. For $N = 4, 5$ there are three different l subspaces: $l_{\max}$, $l_{\max} - 1$ and $l_{\max} - 2$. Thus for $N = 4, 5$ the subspace $l_{\max} - 2$ corresponds to the most subradiant subspace i.e. $N = 4$: $l_{\min} = 4/2 - 2 = 0$ and $N = 5$: $l_{\min} = 1/2$. In these two cases the collective increase in

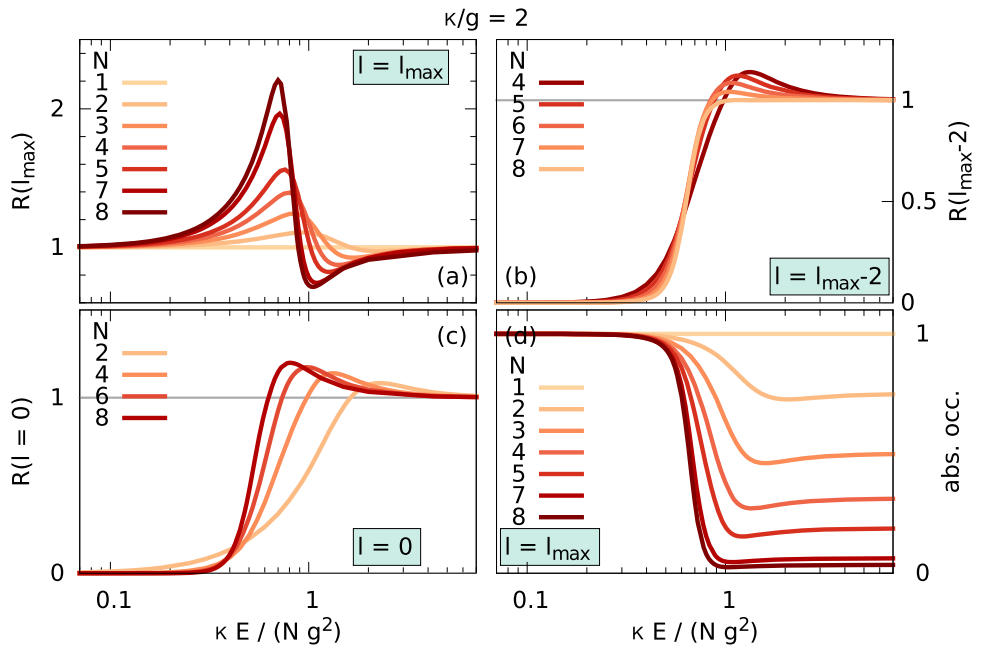

Figure 3. Increasing the system size: relative Dicke subspace occupation for varying N: (a) the superradiant subspace $l = N/2$, (b) $l = N/2 - 2$, (c) $l = 0$. These states have no interactions due to the Hamiltonian. They only couple to states with $l > 0$ through decay and dephasing. (d) Absolute occupation in the superradiant subspace: approaching zero above the phase transition for $N \to \infty$, even without correlations.

population is strongest. For larger N subspaces with smaller l exist, e.g. $N = 6$: $l_{\min} = l_{\max} - 3$. Looking at $R(0)$ (only defined for even N, always corresponds to the most subradiant subspace), figure 3(c), we see that the increase due to collective effects increases with N. Hence the collective increase is always most pronounced in the most subradiant subspace ($l_{\min}$) above the phase transition. Remarkably, below the phase transition the subradiant subspaces are completely suppressed, see figures 3(b), (c).

The total occupation in the superradiant subspace goes to zero above the phase transition for $N \to \infty$, figure 3(d). Naively we could associate this with subradiance. However for $E \to \infty$ the TLS are in a completely incoherent, equipartitioned state [51] and the superradiant subspace is only depopulated since this subspace becomes very small compared to the full Hilbert (Liouville) space for large N. This is clearly not a collective effect. This illustrates that (in the steady state) it is impossible to distinguish between collective and individual behaviour by using Dicke state occupations alone.

However by looking at both the absolute and relative populations we conclude that in the good cavity and large N limit the system changes from a predominantly superradiant to a predominantly subradiant state at the phase transition. This constitutes the main result of this work.

In figure 4 the scaling of experimentally more accessible quantities with the number of individual TLS N is presented: the normalized TLS excitation develops a kink for increasing N, indicating a second-order transition, figure 4(a). The smallest magnitude nonzero eigenvalue λ_1 of the Liouville operator $\mathcal{L}$ (see equation (2)), which corresponds to the slowest time scale in the system to reach steady state, decreases around the phase transition for increasing N, figure 4(b). It might even vanish for $N \to \infty$, creating a second steady state. This could be measured for instance in a hysteresis cycle typical for optical bistability experiments [19, 40, 52]. The intracavity mean photon number shows the formation of a local minimum at the transition and an increase in the peak intensity, figure 4(c). Also bunching ($g^{(2)}(0) > 1$) increases for increasing N, figure 4(d). Overall the transition becomes sharper and more pronounced for increasing N and decreasing κ/g, since these parameters increase the system size. This displays a typical property of phase transitions, which are well defined only in the thermodynamic limit (infinite system size) and blur for small system sizes [4, 53, 54].

5.2. Robustness test, entanglement and the spontaneous decay time

So far all results were presented without including pure dephasing. Now we investigate the robustness of the collective effects at the phase transition against pure dephasing: in figure 5(a) we see that the collective behaviour of the relative Dicke subspace population is reduced for increasing δ. However the effect of clear distinction of superradiant state below and subradiant state above phase transition is preserved for $\delta \sim \gamma$. The general trend of total Dicke subspace occupation is not affected by pure dephasing, as in figure 3(d).

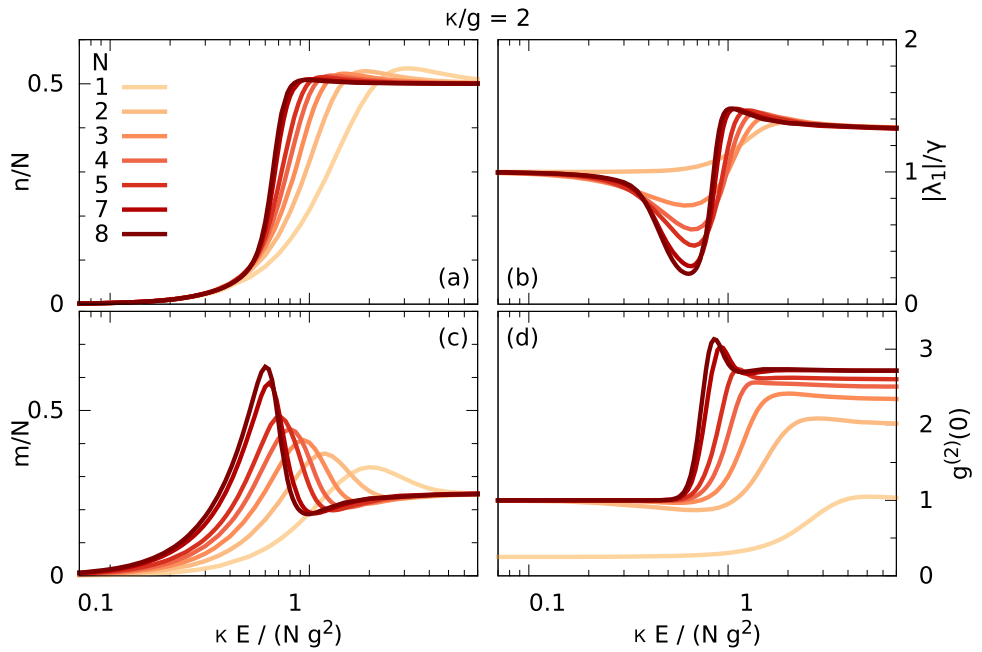

Figure 4. Experimental signatures for varying N: (a) the normalized TLS excitation number $n/N = \langle J_{11}\rangle/N$, (b) the renormalized Liouvillian gap $|\lambda_1|/\gamma$, (c) the rescaled intracavity photon number $m/N = \langle b^\dagger b\rangle/N$ and (d) the second order correlation $g^{(2)}(0)$.

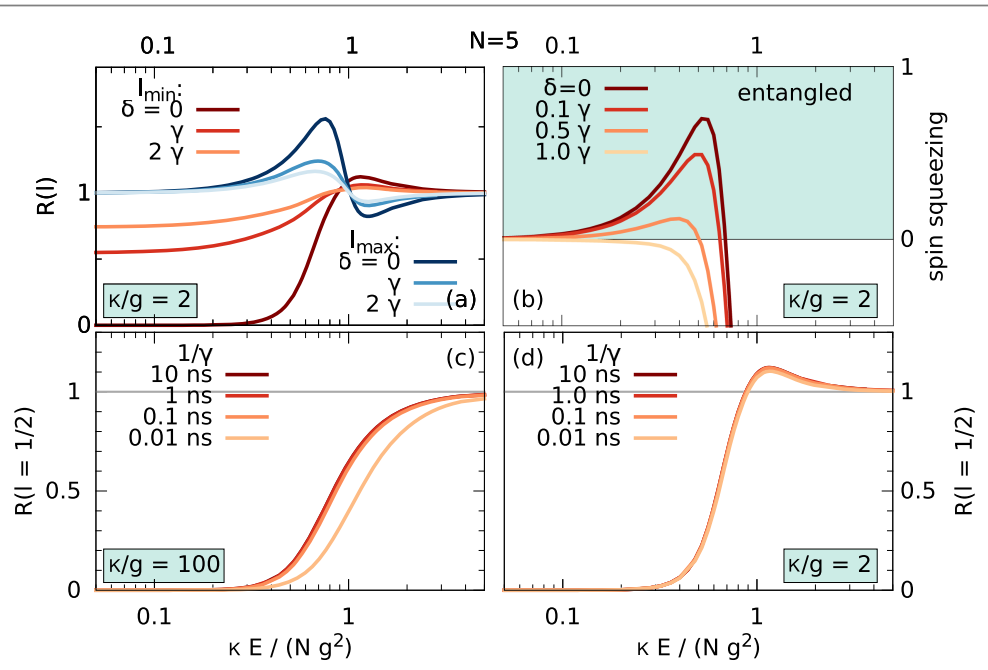

Figure 5. Robustness, entanglement and decay time: (a) the ratio $R(l)$ for $N = 5$ for $l = l_{\min}$, $l_{\max}$ and varying δ: the clear switching at the phase transition survives for $\delta \sim \gamma$. (b) Entanglement via spin squeezing inequalities: entanglement below the transition for $\delta < \gamma$. (c) and (d) The influence of the spontaneous decay time on the population of subradiant states is negligible in realistic parameter ranges. This is especially surprising since this parameter is the only parameter that couples the different Dicke subspaces (for $\delta = 0$). The corresponding ratio γ/g correspond to the interval 2×10^{-5}–2×10^{-2}.

In the spin preserving setup the TLS are entangled via spin squeezing below the phase transition [17]. Spin squeezing is a concept originating from quantum metrology, where it was developed around the idea that squeezed atomic coherent states could be used for measurement precision below the shot noise limit, but also has attracted a lot of attention as an entanglement witness [55–58]. Here we employ the spin squeezing inequalities (SSI) introduced by Tóth *et al* that are explicitly derived as an entanglement witness for many two- (and multi-) level system setups [59, 60]. The spin preserving case does not contain any subradiant states/effects and cannot model the effects of pure dephasing. The spin preserving and nonpreserving scenarios are two limits

of the same physical system [31, 61]. Thus an investigation of entanglement in our setup and its preservation under dephasing is desirable: we find that the SSI by Tóth *et al* detect entanglement below the phase transition for $\delta < \gamma$, see figure 5(b) (see appendix B for the SSI and a definition of the quantity in figure 5(b)). Hence the entanglement detected in the spin preserving setup is still present for spin nonpreserving setups and even for moderate pure dephasing times.

In figures 5(c) and (d) we vary the spontaneous decay time over typical parameter ranges for quantum optics and quantum information setups, such as quantum dots, NV centres and Rydberg atoms. The quantity shown is the relative subradiant subspace occupation for $N = 5$. There is hardly any effect at all, only in the limit of unrealisticly short decay times there is a visible dependence. The qualitative behaviour, that subradiant states are amplified in a good cavity and are not amplified in a bad cavity, is not influenced at all by this parameter. However setting this parameter to zero would result in a decoupling of the different Dicke subspaces and the $R(1/2)$ curves in figures 5(c) and (d) would be fixed at zero. This seems contradictory that the behaviour of the system for decreasing γ does not converge towards the $\gamma = 0$ scenario. This contradiction can be removed by remembering that these results correspond to the *steady state*. In figure 4(b) the renormalized Liouvillian gap λ_l/γ is shown. This gap scales with γ, meaning that with decreasing γ the steady state convergence time increases and becomes infinite for $\gamma \to 0$. Thus this particular steady state will never be reached. This corresponds to a dissipative phase transition, the Liouvillian gap closes, and the different Dicke subspaces form non-interacting subspaces in Hilbert/Liouville space. Thus in this limit the setup is truly multistable with the dimension of the Liouvillian null space being equal to the number of distinct l values.

In summary the spontaneous decay time is a necessary condition for the population of dark states in the system but has no influence on the actual steady state in realistic parameter ranges—γ just scales the time necessary to reach this steady state. Therefore we conclude that—for a finite γ—the only parameter responsible for the dark state coherences and the superradiant to subradiant switching is in fact the cavity quality, which however does not lead to the population of dark states by itself. Therefore the presented effect is a highly nontrivial emergent property, arsing as an interplay of dissipative, individual and coherent, collective, cavity processes.

5.3. Dark state cascades

Super- and subradiance are concepts related to time evolution and so far we have only discussed the steady state: now, we drive the system to the steady state with maximum $R(l_{\min})$ (see figures 3(b) and (c)) and then, afterwards, we switch off the driving field. The system relaxes into the ground state and we observe that a cascade of dark states is generated, figure 6(a): $p(1/2, -1/2)$ and $p(3/2, -3/2)$ are the populations in the lowest states of the smallest $l = l_{\min}$ and intermediate $l_{\max} > l > l_{\min}$ subspace for $N = 5$ TLS (see also figure 1(b)). Both states are dark. They are populated on time scales of the inverse TLS-photon coupling constant g^{-1}, because the higher energy, bright states of the associated l subspaces decay via the emission of cavity photons. The cavity photons subsequently leave the cavity through the cavity decay. After the initial fast population of the $|l, -l\rangle$ states due to the TLS cavity interaction the dynamics are governed by spontaneous emission. At this point the only states populated are the lowermost states in each l subspace and the relative population of these states is determined by the relative population of the respective subspaces before switching off the drive. The overall dark state population subsequently decays on the slower time scale $\gamma^{-1} = 5000g^{-1}$ towards the ground state of the TLS ($|5/2, -5/2\rangle$). The decay follows the Dicke state cascade
$p(1/2, -1/2) \to p(3/2, -3/2) \to p(5/2, -5/2)$. In general for different N: all $m > -l$ states relax to the $m = -l$ states on time scales of the inverse TLS-photon coupling constant g^{-1} which is orders of magnitude faster than the decay time γ^{-1}. Subsequently the dark states $|l, -l\rangle$ relax in a cascade to the lower energy, dark states $|l + 1, -l - 1\rangle$ with minimal l on time scales of γ^{-1} towards the ground state $|l_{\max}, -l_{\max}\rangle$, figure 1(b). Please note that the overall occupation in subradiant dark states reaches values close to unity. In figure 6(b) we see that increasing the number of TLS also increases the total dark state occupation during ground state relaxation. Also the single dark state of the most subradiant state does not experience any initial fast population, since there are no higher energy, bright states in this case.

Overall subradiant correlations are clearly dominant in this cascade, since without these correlations the excitation in the TLS would still decay via the TLS–cavity interaction Hamiltonian. The superradiant to subradiant phase transition and the dark state cascade could be exploited for a controlled generation of subradiant states with dark state occupations up to unity.

The sole requirement for the dark state cascade to occur is individualization: the cascade also occurs in the bad cavity limit and strong pure dephasing (also for $\delta \gg \gamma$) limit. The only difference is that the total transient populations are lower but still approach unity for $N \to \infty$: subradiant states are always populated in the presence of external driving as long as individualization is present and the superradiant subspace becomes very small to the total Hilbert/Liouville space for large N. Thus the system will have an increasing population in subradiant states for large N also in the bad cavity and strong dephasing limit. In the case of strong pure

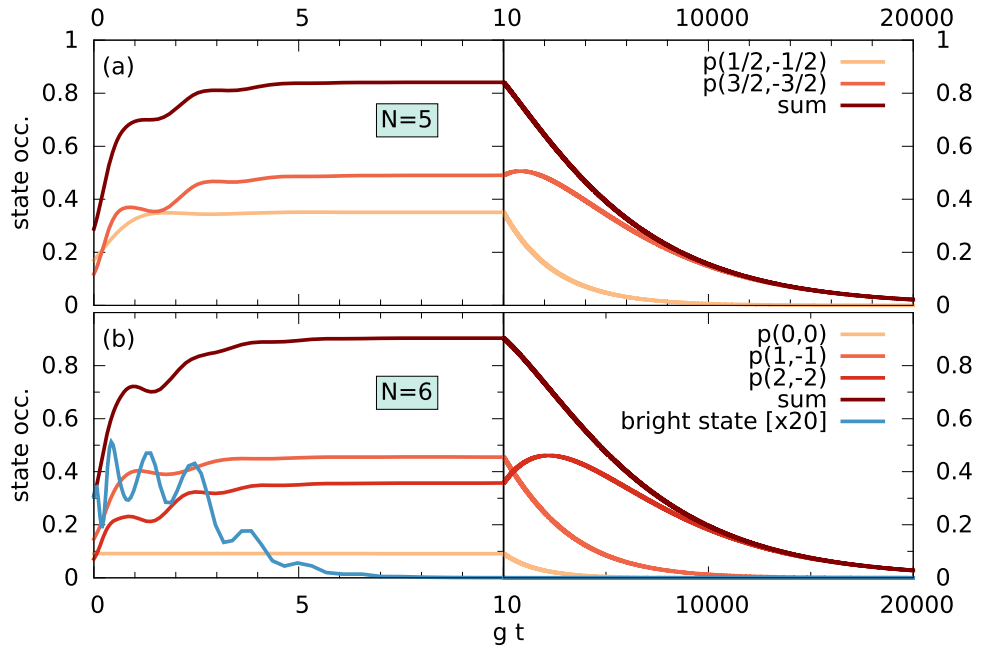

Figure 6. Ground state relaxation and the dark state cascade: (a) driving the system to the maximum subradiance point with subsequent relaxation to the ground state $N = 5$, $\delta = 0$: a cascade of dark states is generated. Total dark state occupation close to unity. (b) Same cascade for $N = 6$: the single dark state of the most subradiant subspace does not experience initial population, since there are no higher energy Dicke states in this subspace. The overall dark state population is higher than for $N = 5$. A single prototypical bright state shows initial Rabi oscillations but decays very fast and remains unpopulated throughout the relaxation process.

dephasing the lifetime of the dark state cascade drops (coherence time). However the effect of favoring subradiant states and the distinction between incoherent/thermal/individual versus quantum coherent/collective two-level system behaviour *in the steady state* relies on the moderate cavity quality and the low pure dephasing.

6. Conclusion

Experimental systems for observing the effects presented in this paper have to meet certain requirements: the pure dephasing of the TLS coherences should be small compared to the decay rate, i.e. $\delta \sim \gamma$. In experimental settings this is usually referred to as lifetime limited coherence time, since then the coherence time in the emitters is essentially limited by the spontaneous radiative lifetime. This can be realized with e.g. Rydberg ensembles [29, 62, 63] or with NV centres [64] and quantum dots [65] at low temperatures. For quantum dots lifetime limited coherence times of 0.63 ns were reported [65]. Also a small inhomogeneous broadening is required, since it would likely blur the presented effect. For quantum dots this is more challenging than for NV centres and Rydberg ensembles. Generally, the decay rate γ is not a crucial parameter but the ratio between decay and pure dephasing. If pure dephasing is too large the steady state effects are blurred, in the ground state relaxation subradiant state occupation is decreased and coherence times are shorter. However the dark state cascade effect is stable even against larger pure dephasing $\delta > \gamma$.

The parameters used in this study are realistic for NV centres, quantum dots and Rydberg atoms and the behaviour is stable over a wide parameter range. Especially varying the spontaneous decay rate γ over realistic parameter ranges has no influence on the discussed effect. For steady state coherences and entanglement properties the relative strength of the pure dephasing δ/γ is crucial, not the absolute value of δ.

In summary we have shown that the nonequilibrium phase transition of cooperative resonance fluorescence changes drastically when leaving the bad cavity limit: subradiant Dicke states are amplified through cavity assisted coherences and clear experimental signatures of this effect emerge. Letting the system relax into the ground state generates a dark state cascade that can be utilized to store quantum information.

Acknowledgments

We thank Nicolas Naumann for useful discussions, and gratefully acknowledge support from the Deutsche Forschungsgemeinschaft (DFG) through SFB 951 (MG, MR, AK) and through the School of Nanophotonics of the SFB 787 (MG) and BR 1528/8-2 (AC, AK).

Appendix A. Details to the permutation symmetric method

The permutation symmetry of the master equation equation (2) confines the dynamics of the density matrix onto the subspace of symmetrized Liouville space states [32, 33, 35, 46]:

$$\hat{\mathcal{P}}[n_{11},\, n_{10},\, n_{01}] = \mathcal{S}\, \sigma_{11}^{\otimes n_{11}} \sigma_{10}^{\otimes n_{10}} \sigma_{01}^{\otimes n_{01}} \sigma_{00}^{\otimes n_{00}}, \tag{A.1}$$

with $n_{00} = N - n_{11} - n_{10} - n_{01}$. The symmetrization operator is defined as $\mathcal{S} = \sum_P \hat{P}$, where $\hat{P}$ is the permutation operator and the sum is over all possible permutations P of two-level systems. This expression is not normalized since the method is numerically more stable without normalization [33]. The density matrix can be expanded in the symmetric states using the Hilbert–Schmidt inner product, tracing over both the photonic and TLS degrees of freedom

$$\mathcal{P}[n_{11},\, n_{10},\, n_{01}] = \mathrm{tr}[\hat{\mathcal{P}}[n_{11},\, n_{10},\, n_{01}]\rho]. \tag{A.2}$$

This corresponds to the pure TLS density matrix. The full degrees of freedom of the present system are given by both TLS and cavity degrees of freedom, therfore for the actual calculations we use the quantities

$$\mathcal{P}[n_{11},\, n_{10},\, n_{01};\, m_l,\, m_r] = \mathrm{tr}[\hat{\mathcal{P}}[n_{11},\, n_{10},\, n_{01}] \otimes |m_l\rangle \langle m_r|\rho], \tag{A.3}$$

including the photonic degrees of freedom with normal bosonic Fock states. Equations of motion can be derived from this expression by taking the time derivative and inserting the quantum master equation. In the PsiQuaSP library this is greatly facilitated by the use of a sketch representation for the symmetric basis states and the action of the Liouville space operators, there no derivation of equations of motion is required [35, 46]. The population in all states outside the symmetric Liouville subspace equation (A.1) is zero, if it is zero in the initial state. Compatible initial states are e.g. the ground state and the thermal equilibrium. The number of different symmetric basis states and thus the overall scaling of the method is $(N+1)(N+2)(N+3)/6 \sim N^3$. For $N = 2$ we retrieve 10 basis states. The $N = 2$ states that occur in the Dicke state expansion are the classical occupation probabilities $\mathcal{P}[0,\, 0,\, 0] = \langle \sigma_{00}^1 \sigma_{00}^2 \rangle$ (TLS ground state), $\mathcal{P}[1,\, 0,\, 0] = \langle \sigma_{11}^1 \sigma_{00}^2 + \sigma_{00}^1 \sigma_{11}^2 \rangle$ (one TLS excited), $\mathcal{P}[2,\, 0,\, 0] = \langle \sigma_{11}^1 \sigma_{11}^2 \rangle$ (both TLS excited) and the quantum correlation $\mathcal{P}[0,\, 1,\, 1] = \langle \sigma_{10}^1 \sigma_{01}^2 + \sigma_{01}^1 \sigma_{10}^2 \rangle$, with $\langle ... \rangle = tr\,[... \rho]$. Exchanging the indices $1 \leftrightarrow 2$ leaves these states invariant—they are permutation symmetric.

Continuing the example for $N = 2$ the expectation values for the Dicke state projectors can be expanded in the symmetrized basis states: $p(1,\, -1) = \mathcal{P}[0,\, 0,\, 0]$, $p(1,\, 0) = 1/2(\mathcal{P}[1,\, 0,\, 0] + \mathcal{P}[0,\, 1,\, 1])$, $p(1,\, 1) = \mathcal{P}[2,\, 0,\, 0]$ and $p(0,\, 0) = 1/2(\mathcal{P}[1,\, 0,\, 0] - \mathcal{P}[0,\, 1,\, 1])$, using the trace condition of [34].

Appendix B. Spin sqeezing inequalities

We employ the SSI introduced by Tóth *et al* [59, 60] as entanglement measure. Tóth *et al* derived seven inequalities that are satisfied by any separable N-qubit state, hence the violation of any of these inequalities implies entanglement. Four of the seven inequalities detect entanglement in our setup, but the violation of two equations is equivalent: the coherent driving field introduces a time dependent phase factor caused by local unitary transformations which do not affect entanglement [66] but cause the violation of the SSI to oscillate back and forth between the two associated inequalities (between (B.1) and (B.2) and between (B.3) and (B.4)). The four SSI that detect entanglement in our setup are

$$\langle J_y^2 \rangle + \langle J_z^2 \rangle - \frac{N}{2} - (N-1)(\Delta J_x)^2 \leqslant 0, \tag{B.1}$$

$$\langle J_x^2 \rangle + \langle J_z^2 \rangle - \frac{N}{2} - (N-1)(\Delta J_y)^2 \leqslant 0, \tag{B.2}$$

$$\langle J_x^2 \rangle + \frac{N(N-2)}{4} - (N-1)[(\Delta J_y)^2 + (\Delta J_z)^2] \leqslant 0, \tag{B.3}$$

$$\langle J_y^2 \rangle + \frac{N(N-2)}{4} - (N-1)[(\Delta J_x)^2 + (\Delta J_z)^2] \leqslant 0, \tag{B.4}$$

where the variances are defined as $(\Delta A)^2 = \langle A^2 \rangle - \langle A \rangle^2$. In order to simplify the discussion we only show one SSI in our plot:

$$\underbrace{\langle J_y^2\rangle + \langle J_z^2\rangle - \frac{N}{2} - (N-1)(\Delta J_x)^2}_{=:A} \leqslant 0, \tag{B.5}$$

hence A is the quantity plotted in figure 5(b). Since strictly speaking the quantities $\langle J_y^2\rangle$ and $\langle J_x^2\rangle$ do not have a defined steady state, but oscillate with the phase factor mentioned above, we set $t = 0$ and thus set the phase factor to unity throughout the plot in figure 5(d). Since, as stated above, the local unitary transformations causing the oscillation do not affect the entanglement, this is a valid approach. In the following the local unitary transformation is explained:

On resonance the Hamiltonian of the system in a frame rotating at the external laser frequency ω_l reads

$$H = g(J_{10}b + J_{01}b^\dagger) + E(J_{10} + J_{01}). \tag{B.6}$$

The corresponding master equation for the setup considered in this work is

$$\partial_t\rho = \mathcal{L}\rho = \frac{\mathrm{i}}{\hbar}[\rho, H] + \mathcal{D}_{\mathrm{de}} + \mathcal{D}_{\mathrm{pd}} + \mathcal{D}_{\mathrm{ph}}, \tag{B.7}$$

where ρ is the rotating frame density matrix. The transformation between normal frame and rotating frame is given by

$$\rho_n = \mathrm{e}^{-\frac{\mathrm{i}}{\hbar}H_{\mathrm{rot}}t}\rho\mathrm{e}^{\frac{\mathrm{i}}{\hbar}H_{\mathrm{rot}}t}, \tag{B.8}$$

with the normal frame density matrix ρ_n and the Hamiltonian

$$H_{\mathrm{rot}} = \hbar\omega_l(b^\dagger b + J_{11}). \tag{B.9}$$

The Hamiltonian acts locally on the density matrix, in the sense that each TLS experiences an individual unitary transformation, i.e.

$$\mathrm{e}^{J_{11}} = \prod_{i=1}^{N} \mathrm{e}^{\sigma_{11}^i}. \tag{B.10}$$

Such a transformation leaves the quantum correlations invariant [66]. Nonetheless some quantities arising in the SSI experience a time dependency through this transformation. In fact only the rotating frame density matrix has a stationary steady state, the normal frame density matrix ρ_n exhibits an oscillating steady state, where diagonal entries are stationary and offdiagonal entries oscillate with a phase of multiples of ω_l.

The quantities $\langle J_{x,y}^2\rangle$ and $(\Delta J_{x,y})^2$ are explicitly time dependent in the normal frame. By adding equations (B.1)–(B.4) respectively, one can derive time independent inequalities, which however do not detect entanglement in our setup.

ORCID iDs

Marten Richter https://orcid.org/0000-0003-4160-1008

References

[1] Dicke R H 1954 Coherence in spontaneous radiation processes *Phys. Rev.* **93** 99–110
[2] Garraway B M 2011 The Dicke model in quantum optics: Dicke model revisited *Phil. Trans.* A **369** 1137–55
[3] Wang Y K and Hioe F T 1973 Phase transition in the Dicke model of superradiance *Phys. Rev.* A **7** 831
[4] Walls D F, Drummond P D, Hassan S S and Carmichael H J 1978 Non-equilibrium phase transitions in cooperative atomic systems *Suppl. Prog. Theor. Phys.* **64** 307
[5] Narducci L M, Feng D H, Gilmore R and Agarwal G S 1978 Transient and steady-state behavior of collective atomic systems driven by a classical field *Phys. Rev.* A **18** 1571
[6] Carmichael H J 1980 Analytical and numerical results for the steady state in cooperative resonance flourescence *J. Phys. B: At. Mol. Phys.* **13** 3551
[7] Drummond P D and Walls D F 1981 Quantum theory of optical bistability: II. Atomic flourescence in a high-Q cavity *Phys. Rev.* A **23** 2563
[8] Puri R R and Lawande S V 1979 Exact steady-state density operator for a collective atomic system in an external field *Phys. Lett.* A **72** 200–2
[9] Hassan S S, Bullough R K, Puri R R and Lawande S V 1980 Intensity fluctuations in a driven Dicke model *Phys.* A **103** 213
[10] Lawande S V, Puri R R and Hassan S S 1981 Non-resonant effects in the fluorescent Dicke model: I. Exact steady state analysis *J. Phys. B: At. Mol. Phys.* **14** 4171
[11] Sarkar S and Satchell J S 1987 Solution of master equations for small bistable systems *J. Phys. A: Math. Gen.* **20** 2147
[12] Sarkar S and Satchell J S 1987 Optical bistability with small numbers of atoms *Europhys. Lett.* **3** 797
[13] Clive E and Brandes T 2003 Quantum chaos triggered by precursors of a quantum phase transition: the Dicke model *Phys. Rev. Lett.* **90** 044101
[14] Schneider S and Milburn G J 2002 Entanglement in the steady state of a collective-angular-momentum (Dicke) model *Phys. Rev.* A **65** 042107
[15] Schneebeli L, Kira M and Koch S W 2008 Characterization of strong light-matter coupling in semiconductor quantum-dot microcavities via photon-statistics spectroscopy *Phys. Rev. Lett.* **101** 097401

[16] Lee T E, Häffner H and Cross M C 2012 Collective quantum jumps of Rydberg atoms *Phys. Rev. Lett.* **108** 023602
[17] González-Tudela A and Porras D 2013 Mesoscopic entanglement induced by spontaneous emission in solid-state quantum optics *Phys. Rev. Lett.* **110** 080502
[18] Su Y, Bimberg D, Knorr A and Carmele A 2013 Collective light emission revisited: reservoir induced coherence *Phys. Rev. Lett.* **110** 113604
[19] Carr C, Ritter R, Wade C G, Adams C S and Weatherill K J 2013 Nonequilibrium phase transition in a dilute Rydberg ensemble *Phys. Rev. Lett.* **111** 113901
[20] Genway S, Li W, Ates C, Lanyon B P and Lesanovsky I 2014 Generalized Dicke nonequilibrium dynamics in trapped ions *Phys. Rev. Lett.* **112** 023603
[21] Zou L J, Marcos D, Diehl S, Putz S, Schmiedmayer J, Majer J and Rabl P 2014 Implementation of the Dicke lattice model in hybrid quantum system arrays *Phys. Rev. Lett.* **113** 023603
[22] Richter M, Gegg M, Theuerholz T S and Knorr A 2015 Numerically exact solution of the many emitter-cavity laser problem: application to the fully quantized spaser emission *Phys. Rev.* B **91** 035306
[23] Wolfe E and Yelin S F 2014 Certifying separability in symmetric mixed states of n qubits, and superradiance *Phys. Rev. Lett.* **112** 140402
[24] Scully M O 2015 Single photon subradiance: quantum control of spontaneous emission and ultrafast readout *Phys. Rev. Lett.* **115** 243602
[25] Cong K, Zhang Q, Wang Y, Noe G T, Belyanin A and Kono J 2016 Dicke superradiance in solids *J. Opt. Soc. Am.* B **33** C80–101
[26] Kirton P and Keeling J 2017 Suppressing and restoring the Dicke superradiance transition by dephasing and decay *Phys. Rev. Lett.* **118** 123602
[27] Shammah N, Lambert N, Nori F and De Liberato S 2017 Superradiance with local phase-breaking effects *Phys. Rev.* A **96** 023863
[28] Pleinert M-O, von Zanthier J and Agarwal G S 2017 Hyperradiance from collective behavior of coherently driven atoms *Optica* **4** 779
[29] Guerin W, Araújo M O and Kaiser R 2016 Subradiance in a large cloud of cold atoms *Phys. Rev. Lett.* **116** 083601
[30] Martini U and Schenzle A 2001 Cavity QED with many atoms *Directions in Quantum Optics: A Collection of Papers Dedicated to the Memory of Dan Walls Including Papers Presented at the TAMU-ONR Workshop Held at Jackson, Wyoming, USA, 26–30 July 1999* ed H J Carmichael, R J Glauber and M O Scully (Berlin: Springer) pp 238–49
[31] Carmichael H J 2002 *Statistical Methods in Quantum Optics I: Master Equations and Fokker–Planck Equations* (Berlin: Springer)
[32] Hartmann S 2016 Generalized Dicke states *Quantum Inf. Comput.* **16** 1333–48
[33] Gegg M and Richter M 2016 Efficient and exact numerical approach for many multi-level systems in open system CQED *New J. Phys.* **18** 043037
[34] Xu M, Tieri D A and Holland M J 2013 Simulating open quantum systems by applying su(4) to quantum master equations *Phys. Rev.* A **87** 062101
[35] Gegg M and Richter M 2017 Psiquasp—a library for efficient computation of symmetric open quantum systems *Sci. Rep.* **7** 16304
[36] Carmichael H J, Satchell J S and Sarkar S 1986 Nonlinear analysis of quantum fluctuations in absorptive optical bistability *Phys. Rev.* A **34** 3166
[37] Breuer H-P and Petruccione F 2002 *The Theory of Open Quantum Systems* (Oxford: Oxford University Press)
[38] Mandel L and Wolf E 1995 *Optical Coherence and Quantum Optics* (Cambridge: Cambridge University Press)
[39] Gibbs H M 1985 *Optical Bistability: Controlling Light with Light* (New York: Academic)
[40] Rodriguez S R K *et al* 2017 Dynamic optical hysteresis in the quantum regime *Phys. Rev. Lett.* **118** 247402
[41] Schenzle A and Brand H 1979 Dynamic behaviour of optical bistability *Opt. Commun.* **31** 401
[42] Kessler E M, Giedke G, Imamoglu A, Yelin S F, Lukin M D and Cirac J I 2012 Dissipative phase transition in a central spin system *Phys. Rev.* A **86** 012116
[43] Drummond P D and Gardiner C W 1980 Generalised p-representations in quantum optics *J. Phys. A: Math. Gen.* **13** 2353
[44] Chase B A and Geremia J M 2008 Collective processes of an ensemble of spin-1/2 particles *Phys. Rev.* A **78** 052101
[45] Baragiola B Q, Chase B A and Geremia J M 2010 Collective uncertainty in partially polarized and partially decohered spin-1 2 systems *Phys. Rev.* A **81** 032104
[46] Gegg M and Richter M 2017 Psiqua SP—permutation symmetry for identical quantum systems package (https://github.com/modmido/psiquasp)
[47] Balay S *et al* 2017 (http://www.mcs.anl.gov/petsc)
[48] Balay S 2016 PETSc users manual *Technical Report* ANL-95/11 Argonne National Laboratory Revision 3.7(http://www.mcs.anl.gov/petsc)
[49] Balay S, Gropp W D, McInnes L C and Smith B F 1997 Efficient management of parallelism in object oriented numerical software libraries *Modern Software Tools in Scientific Computing* ed E Arge *et al* (Boston, MA: Birkhäuser Press) pp 163–202
[50] Hernandez V, Roman J E and Vidal V 2005 SLEPc: a scalable and flexible toolkit for the solution of eigenvalue problems *ACM Trans. Math. Softw.* **31** 351–62
[51] Richter M, Renger T, Renger G and Knorr A 2007 Nonperturbative theory for the optical response to strong light of the light harvesting complex II of plants: saturation of the fluorescence quantum yield *J. Chem. Phys.* **127** 075105
[52] Gibbs H M, McCall S L and Venkatesan T N C 1976 Differential gain and bistability using a sodium-filled Fabry–Perot interferometer *Phys. Rev. Lett.* **36** 1135
[53] Rice P R and Carmichael H J 1994 Photon statistics of a cavity-QED laser: a comment on the laser phase-transition analogy *Phys. Rev.* A **50** 4318
[54] Gross D H E 2001 *Microcanonical Thermodynamics: Phase Transitions in 'Small' Systems* (Singapore: World Scientific)
[55] Wineland D J, Bollinger J J, Itano W M, Moore F L and Heinzen D J 1992 Spin squeezing and reduced quantum noise in spectroscopy *Phys. Rev.* A **46** R6797
[56] Wineland D J, Bollinger J J, Itano W M and Heinzen D J 1994 Squeezed atomic states and projection noise in spectroscopy *Phys. Rev.* A **50** 67
[57] Kitagawa M and Ueda M 1993 Squeezed spin states *Phys. Rev.* A **47** 5138
[58] Dylewsky D, Freericks J K, Wall M L, Rey A M and Foss-Feig M 2016 Nonperturbative calculation of phonon effects on spin squeezing *Phys. Rev.* A **93** 013415
[59] Tóth G, Knapp C, Gühne O and Briegel H J 2007 Optimal spin squeezing inequalities detect bound entanglement in spin models *Phys. Rev. Lett.* **99** 250405
[60] Tóth G, Knapp C, Gühne O and Briegel H J 2009 Spin squeezing and entanglement *Phys. Rev.* A **79** 042334
[61] Agarwal G S 1974 Quantum statistical theories of spontaneous emission and their relation to other approaches *Quantum Optics. Springer Tracts in Modern Physics* vol 70 (Berlin: Springer) pp 1–128

[62] Pritchard J D, Maxwell D, Gauguet A, Weatherill K J, Jones M P A and Adams C S 2010 Cooperative atom-light interaction in a blockaded Rydberg ensemble *Phys. Rev. Lett.* **105** 193603
[63] Saffman M, Walker T G and Mølmer K 2010 Quantum information with Rydberg atoms *Rev. Mod. Phys.* **82** 2313
[64] Tamarat P *et al* 2006 Stark shift control of single optical centers in diamond *Phys. Rev. Lett.* **97** 083002
[65] Borri P, Langbein W, Schneider S, Woggon U, Sellin R L, Ouyang D and Bimberg D 2001 Ultralong dephasing time in ingaas quantum dots *Phys. Rev. Lett.* **87** 157401
[66] Vedral V, Plenio M B, Rippin M A and Knight P L 1997 Quantifying entanglement *Phys. Rev. Lett.* **78** 2275